

BTS-VNET: BRAIN TUMOUR SEGMENTATION VIA DEEP LEARNING BASED DUAL ATTENTION INTEGRATED V-NETWORK

S. Prathiba¹ and B. Sivagami²

¹Research Scholar, Department of Computer Science & Research Centre, S.T. Hindu College, Nagercoil – 629002, Affiliated to Manonmaniam Sundaranar University, Abishekapatti, Tirunelveli – 627012, Tamil Nadu, India.

²Associate Professor, Department of Computer Science & Application, S.T. Hindu College, Nagercoil – 629002, Affiliated to Manonmaniam Sundaranar University, Abishekapatti, Tirunelveli – 627012, Tamil Nadu, India.

Corresponding author: S. Prathiba (prathibasuyambu26@gmail.com).

Abstract

Brain tumor occurs when abnormal cells form within the brain. There are two main types of tumors: malignant (cancerous) tumors and benign (non-cancerous). Brain Tumor Segmentation (BTS) is a medical image analysis task that involves the separation of brain tumors from normal brain tissue in magnetic resonance imaging (MRI) scans. Segmenting tumor automatically in human brain MRI images is challenging because of uneven, irregular and unstructured size and shape of the tumor. In this paper, a novel BTS-VNET has been proposed for brain tumor detection and segmentation using a deep learning approach. The process begins with input MRI scans that undergo pre-processing steps, including skull stripping and scalable range based adaptive bilateral filter (SCRAB) for removing the noisy artifacts. The pre-processed images are then passed through a Dilated Regularized Network for initial tumor detection for classifying the MRI images as either normal or abnormal. Afterwards, the abnormal images are fed into the tumor segmentation phase using a Dual Attention V-Network for resulting in segmented output that contains tumor regions. The proposed method is evaluated in terms of FScore, sensitivity, time taken, Segmentation Accuracy (SA), Average Misclassification Ratio (AMR), and Eye Perception-based Quality Index (EPQI).

Keywords: Brain tumor segmentation, SCRAB filter, Dilated Regularized Network, Dual Attention V-Network, Magnetic Resonance Imaging (MRI).

1. INTRODUCTION

A brain tumor is defined as the proliferation of aberrant cells inside the skull. Because it is stiff, this abnormal development inside the skull causes problems. There are two primary forms of brain tumors. The benign tumor, which is not cancerous, and the malignant tumor, which is cancerous. Any additional brain cell growth may cause pressure inside the skull. [1]. The symptoms of brain tumors might vary depending on the area of the brain that is affected. Seizures, nausea, headaches, mental difficulties and blurred vision are a few examples of these symptoms. One of the scariest diseases that may strike anyone at any age or gender is a brain tumor. Children are experiencing it more frequently, which may be related to their increased use of technology, including tablets, smartphones, and other gadgets [2]. To fully study the structure of the brain, a variety of imaging modalities are used such as computed tomography (CT), positron emission tomography (PET) and magnetic resonance imaging (MRI). When compared PET and CT, MRI is thought to be superior [3]. The most common form of brain tumor formed from glial cells is glioma. According to the world health organization (WHO), tumor behaviors and microscopic images can be used to categorize gliomas into four distinct stages [4]. A deep learning (DL) model has multiple processing layers that represent data in a variety of abstractions. Nearly all fields employ DL, but biostatistics and medical imaging particularly do. Consequently, deep learning has greatly enhanced the ability to identify, forecast, and perform diagnostic tests in a number of medical domains, such as pathology, brain tumors, lung disease,

the stomach, the cardiovascular system, and the retina [5]. Deep neural networks that can segment and classify images are called convolutional neural networks (CNNs). A range of distinct layers, each serving a particular function, are included in CNN designs for classification and segmentation, including dropout layers, convolutional layers, pooling layers, fully connected layers and so on [6].

The following are the most common four categories of brain tumors: Meningitis Since these tumors originate in the meninges, the membranes lining the skull and spinal canal, they are not truly brain tumors. However, their growth may have an adverse effect on the brain, leading to a variety of problems like memory loss, hearing and visual impairment, or even convulsions. Tumors that originate from glial cells are known as gliomas. Normal functions of these cells include supporting the structure of the central nervous system, feeding it, eliminating waste from the body, breaking down dead neurons, and potentially developing gliomas from various glial cell types. Cancer of the breast or lung causes metastatic brain tumors, the most common type of adult brain tumor. Astrocytomas are primary tumors that start in astrocytes, star-shaped cells found in the cerebrum of the brain [7]. Brain tumor identification requires the use of segmentation techniques. There are two methods for segmentation: automatic and manual. Whereas automatic segmentation uses histograms based on pixel intensities, manual segmentation reduces computational efficiency and takes more effort and expert expertise [8].

This paper proposes a new approach for brain tumor detection and segmentation. The key contributions of this model are outlined below,

The purpose of this study is to provide a BTS-VNET for brain tumor segmentation.

The process begins with input MRI scans that undergo pre-processing steps, including skull stripping and SCRAB filter for removing the noisy artifacts.

The pre-processed images are then passed through a Dilated Regularized Network for initial tumor detection for classifying the MRI images as either normal or abnormal.

The abnormal images are fed into the tumor detection segmentation phase using a Dual Attention V-Network for resulting in segmented output that segments different tumor regions.

The proposed method is evaluated in terms of FScore, sensitivity, time taken, SA, AMR, and eye perception-based quality index (EPQI).

The structure of the paper is planned as follows: Section two offers a literature survey, Section three presents the proposed system, Section four presents the results and discussion and Section five includes the conclusion and future work.

2 LITERATURE SURVEY

In recent years, several researches have investigated for the classification of brain tumor segmentation with deep neural network and ML methods. The section that follows provides a review of some current research papers.

In 2019, Ding et al [9] proposed a framework called Stack Multi-Connection Simple Reducing Net to segment the brain tumor region in MRI images. Herein, some bridge connections, which are used to make full use of the information, have also been developed to build a series of bridges inside the cascade network. The goodness of this model is that it can extract the brain tumor boundary in a better manner. But the major pitfall of this model is that it loses its efficiency when it is applied to segment different types of brain images.

In 2020, Gawad et al [10] proposed an enhanced edge detection technique based on a genetic algorithm to aid brain tumor segmentation. This algorithm considers numerous training images and their corresponding adequate edge images, which in turn yields an optimal edge filter and thresholding algorithm. The benefit of this technique is that it provides better localization and detects sharper edges in an efficient manner. On the other hand, since this technique has been trained with brain MRI images of a particular noise level, it loses credibility while segmenting images with huge noise level.

In 2021, Gunasekara et al [11] proposed a methodical technique that uses active contouring and DL for MRI brain tumor segmentation and localization. For the purpose of segmentation, the tumor borders were found using the Chan–Vese technique. In order to locate the tumor regions of interest in the categorized images, a region-based convolutional neural network (R-CNN) is applied after classifiers using a deep CNN are first developed. With an average Dice Score of 92%, the proposed design performs well overall for both glioma and meningioma segmentation, indicating its excellent dependability.

In 2020, Jia, Z. and Chen [12] proposed the use of DL approaches for the identification and categorization of brain tumors in MRI images. It is difficult to identify aberrant

structures in the human brain using standard imaging methods. The probabilistic neural network classification method has been used to train and validate the tumor detection accuracy in brain MRI images. The probabilistic neural network classification method has been used to train and validate the tumor detection accuracy in brain MRI images. The numerical findings illustrate the effectiveness of the suggested system, with nearly 98.51% accuracy in distinguishing between diseased and normal tissue from brain magnetic resonance scans.

In 2022, Khan et al [13] proposed a DL based intelligent model for the detection of brain tumors. CNN is utilized in the proposed hierarchical DL based brain tumor (HDL2BT) classification system for brain tumor identification and categorization. For a prompt and effective cure, the diagnosis and tumor classification are crucial, and CNN are producing excellent results in medical image processing. Gliomas, meningiomas, pituitary tumors, and no tumor are the four categories into which the proposed approach divides the tumor. The proposed model outperforms previous techniques for brain tumor detection and segmentation, with 92.13% precision and a 7.87% miss rate.

In 2021, Ejaz et al [14] proposed an improved Sobel edge detection algorithm that extracts the brain tumor region in a better manner. Herein, it uses a hybrid segmentation technique to segment the tumor area from the input image. The advantage of this hybrid segmentation algorithm is that it shows better efficiency in segmenting the tumor region from a brain tumor dataset. At the same time, the stumbling block of this technique is that it loses its efficacy while segmenting the tumor region with uncertainty due to the use of hard thresholds in tumor segmentation.

In 2020, Yaqub et al [15] proposed a CNN optimizer to separate brain tumors from other images using magnetic resonance imaging. CNN behave differently depending on a variety of criteria, including the quality of the input and particular combinations of these model properties. A thorough comparison study of well-known CNN optimizers to benchmark segmentation for enhancement. The BraTS2015 data collection was used for the experiments. When it came to improving CNN's capacity for segmentation and classification, the Adam optimizer achieved the highest accuracy rate of 99.2%.

In 2022, ZainEldin et al [16] proposed a CNN-based Brain Tumor Classification Model (BCMCNN), which uses the adaptive dynamic sine-cosine fitness grey wolf optimizer (ADSCFGWO) method to improve CNN hyperparameters. The model improves brain tumor diagnosis by using widely used pre-trained models (Inception-ResnetV2). Its output is a binary 0 or 1 (0: Normal, 1: Tumor). The findings of the experiment demonstrate that the BCM-CNN classifier produced the best results since the hyperparameters of the CNN optimization improved the CNN's performance. Using the BRaTS 2021 dataset, the accuracy of the BCM-CNN is 99.98%.

In 2022, Vankdothu, R. and Hameed [17] proposed a brand-new automatic detection and categorization system. Better classification outcomes for brain images from a given input dataset are obtained using the proposed strategy. The studies were carried out using 2870 training set MRI images and 394 testing sets from the Kaggle dataset. The outcomes show that the proposed strategy outperforms earlier approaches in terms of performance. Lastly, a comparison is made between the

present RCNN, U-Net, and BP classification methods and the suggested RCNN method. The proposed classifier classified brain tumor tissues from MRI images with 95.17% accuracy.

In 2021, Guan et al [18] proposed a powerful tumor grading instrument on a brain tumor dataset that is accessible to the public. The proposed strategy outperformed the other approaches assessed on the same dataset, according to extensive experiment results, and it obtained an optimal performance with an overall classification accuracy of 98.04%. Additionally, the model produced results for the Meningioma, Glioma, and Pituitary classes that were 99.17, 98.66, and 99.24% accurate, 96.89, 97.82, and 99.24% sensitive (recall), and 98.55, 99.38, and 99.25% specific.

In 2024, Nassar et al [19] proposed a reliable hybrid DL method for classifying brain tumors based on MRI data. The accuracy and speed of diagnosis in the field of magnetic resonance imaging (MRI)-based tumor detection and classification, particularly in the case of brain tumors, are greatly aided by the application of DL. In an attempt to leverage the combined power of several models and provide encouraging outcomes, the proposed approach is based on the output of five distinct models. The findings have significantly improved thanks to the proposed system, which has an overall accuracy of 99.31%.

In 2024, Kumar et al [20] proposed a novel method for conditional synthesis and auxiliary categorization of brain tumors by pre-training using a style-based generative adversarial network. A publicly available magnetic resonance imaging dataset comprising three distinct tumor types—glioma, meningioma, and pituitary—was used to validate the suggested

methodology. This strategy is also advantageous for small and fresh datasets with similar distributions, since transfer learning can make the framework adaptive. The suggested solution outperformed alternative methods, achieving test accuracy, precision, and recall scores of 99.51%, 99.52%, and 99.50%, respectively.

In 2024, Chauhan et al [21] proposed DL models, such as ResNet50, PSPNet, U-Net, and DeepLabV3+, have shown promising results in brain tumor segmentation. Accurate brain tumor segmentation utilizing multi-contrast MRI images is crucial for analysis and therapy planning. Lower performance was attained by the DeepLabV3+ and ResNet50 models, with DSCs of 0.85 and 0.83, respectively. The 3D U-Net model with data augmentation and transfer learning is recommended for brain tumor segmentation using multi-contrast MRI images based on the findings and analysis.

Based on the literature survey above, existing techniques have been developed using various DL and ML approaches for brain tumor segmentation. However, these methods exhibit a low reliability rate due to issues such as time complexity and a limited set of images. To address this challenge, a BTS-VNET model has been proposed for more effective brain tumor segmentation.

3. PROPOSED SYSTEM

In this section, the model has been proposed for brain tumor segmentation. The overall workflow of the BTS-VNET shown in figure 1,

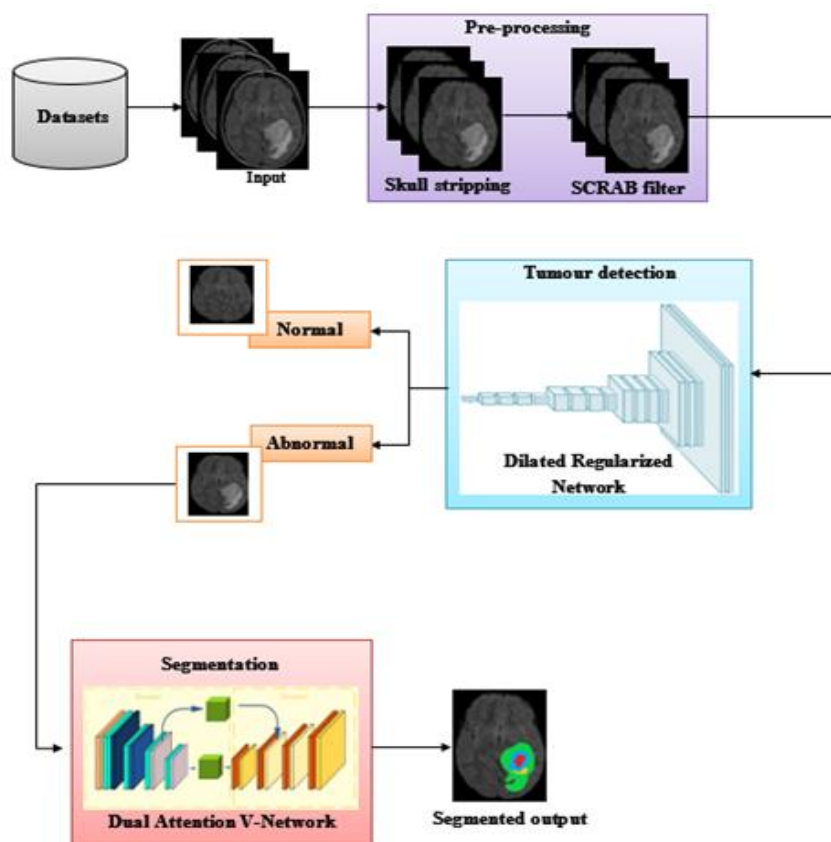


Figure 1: The overall workflow of proposed BTS-VNET

3.1 Dataset description

This research uses the following four databases of MRI brain images:

- MMHRC-DB (MMHRC Database 2021)
- PRNV-DB (PRNV Database 2021)
- NSC-DB (NSC Database 2021)
- SSL-DB (SSL Database 2021).

3.2 Data pre-processing

Pre-processing enhances medical images by eliminating noise and enhancing delicate changes. For the initial analysis of the input MRI images, non-brain tissues are removed from the skull to isolate the brain region. The SCRAB enhances image quality by reducing noise and improving contrast after skull stripping.

3.2.1 Skull stripping

One of the most important phases in the preprocessing of an MRI picture is called "skull stripping," which involves separating the white and gray matter tissues from the skull. Skull stripping must be done precisely to avoid incorrectly estimating the cerebral and cortical thickness of the skull. The accuracy of the geometric assumptions used in the present methods is highly dependent on features that may not be well-designed or may not meet standards due to subpar picture registration. We use Otsu's thresholding technique to determine the image's threshold and apply labels accordingly. The bimodality of the histogram's intensity is assumed by this thresholding technique. If not, a Gaussian averaging filter is utilized to make it into one and smooth the image as well. It produces a very distinct background and foreground by maximizing the inter-class variance and minimizing the intra-class variance. As a result, the image is transformed from grayscale to binary. The following is Otsu's mathematical interpretation:

$$\sigma_w^2(t) = \omega_0(t)\sigma_0^2(t) + \omega_1(t)\sigma_1^2(t) \quad (1)$$

Where the intra-class variance is denoted by $\sigma_w^2(t)$. It is determined by adding together the weighted variance of the two distinct classes. Here's how the separate weights are determined:

$$\omega_0(t) = \sum_{i=0}^{t-1} p(i) \quad (2)$$

$$\omega_1(t) = \sum_{i=t}^{L-1} p(i) \quad (3)$$

The probability of each pixel's intensity is represented by $p(i)$ in this case. According to the following equations, Otsu's technique also demonstrates that maximizing the inter-class variance likewise minimizes the intra-class variation:

$$\sigma_b^2(t) = \sigma^2 - \sigma_w^2(t) \quad (4)$$

Skull stripping for tumor segmentation,

$$\sigma_b^2(t) = \omega_0(\mu_0 - \mu_T)^2 + \omega_1(\mu_1 - \mu_T)^2 \quad (5)$$

$$\sigma_b^2(t) = \omega_0(t)\omega_1(t)[\mu_0(t) - \mu_1(t)]^2 \quad (6)$$

3.2.2 Scalable range based adaptive bilateral filter

An MRI image is processed using the bilateral filter in this phase in order to eliminate noise, level it out, make it nonlinear, and preserve edges. First, the intensity pixel value is determined. Next, the Gaussian distribution function determines the weighted intensity mean of each neighboring pixel. The weights were then ranged using Euclidean distance and radiometric discrepancies. With these numbers, the input image's noise level is reduced while the pixel edges remain intact. One of the bilateral filter's main shortcomings is that it does not collect all of the edge variation data in noisy images. Consequently, the SCRAB filter is employed to rectify this defect and it may be deduced as follows:

$$z_r(p, x, q) = \alpha \exp\left(-\frac{1}{2}\left(\frac{|f(p) - f(x) - q(x)|}{\sigma_r}\right)^2\right) + \beta \quad (7)$$

$$q(x) = \begin{cases} |f(x) - \text{mean}(\Omega_y)| & |p - q| \leq c \\ 0 & \text{otherwise} \end{cases} \quad (8)$$

Where the pixel set of the $(2n+1)*(2n+1)$ pixel window, where $n=2$, is denoted by Ω_y . The average value is Ω_y , the positive parameters are α and β , and the range-based functions $q(x)$ is based on c , a stable variable. The linear constant coefficients $\alpha = 2$ and $\beta = 1$, as well as the scaling factor σ_r are the three parameters that regulate z_r . Out of these three σ_r ensures the higher rate of photometric similarity between x central pixel x and its p neighbouring pixels.

3.3 Tumor detection

Image preprocessing is done before entering the Dilated Regularized Network. Using this network, images are categorized as either "Normal" or "Abnormal." A new paradigm for neural network architecture is represented by RegNet. A residual network was set up to facilitate the deeper network training process. It can demonstrate strong cross-setting generalization capabilities and advance our understanding of design concepts and network architecture. RegNet generates network design spaces that may parameterize whole networks, as opposed to concentrating on the design of individual network instances. The design process is similar to a manually designed network, but it raises the design space level. Consequently, we are able to construct a low dimensional design space containing multiple regular and fundamental networks. RegNet is not a single network, nor is it an extended family of networks like EfficientNets. It is a quantized linearly constrained design space. With the same training design and FLOPs, RegNet is five times faster and performs better in terms of accuracy and GPU throughput than the state-of-the-art (SOTA) EfficientNet. Figure 3 depicts the architecture of the dilated Regularized Network,

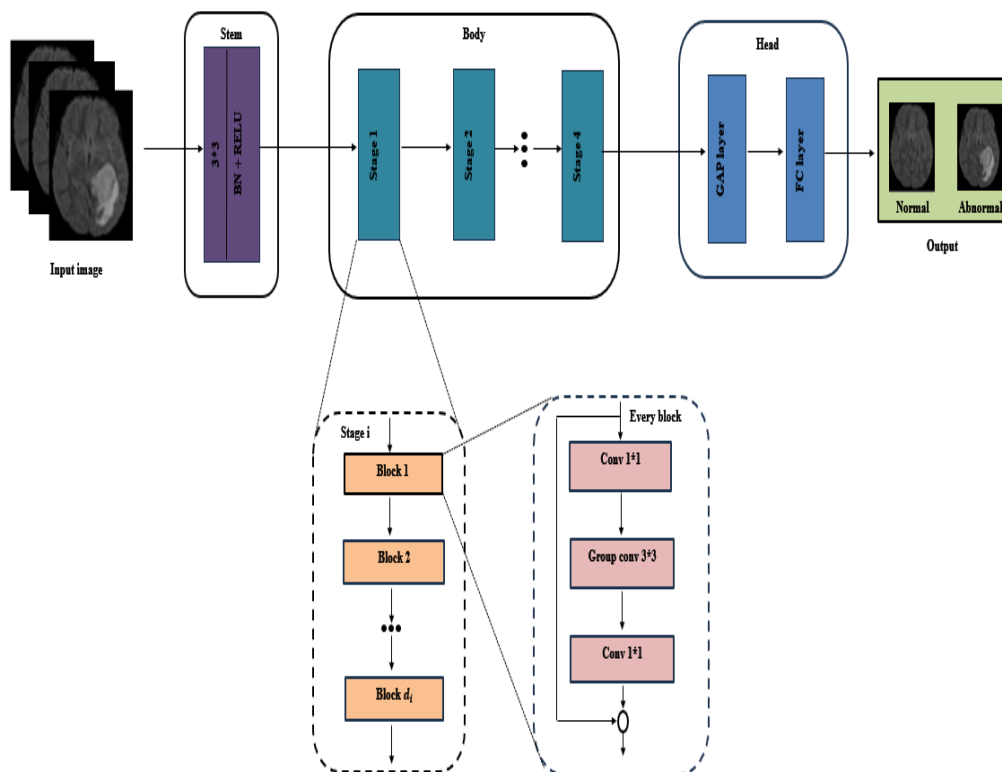


Figure 3: The architecture of Dilated Regularized Network

The stem, body, and head are the three basic components that make up the RegNet network. This network focuses primarily on the structure of the network body, keeping the head network and backbone as basic as possible. The stem is a standard convolution layer that by default includes BN and RELU. The convolution kernel has 32 convolution cores, a step length of 2, and a size of 3×3 . The four phases that make up the body's structure are arranged in a stack. The input characteristic matrix's height and breadth will be cut in half at the end of each step. A sequence of block stacks makes up each step. Group convolutions (on the main branch) and standard convolutions (on the shortcut branch) with a step of two are present in the first block of each stage, whereas the step of the convolutions in the subsequent blocks is 1. A global average pooling layer plus a full connection layer make up the Head classifier, which is a common classifier in the classification network. The RegNet block and the ResNet block are nearly identical. A 3×3 group convolution (containing BN and RELU), a 1×1 convolution (including BN), and a 1×1 convolution (including BN) are the three primary branches. When $stripe = 1$, no processing happens on the shortcut branch. Down sampling is carried out using a 1×1 convolution (including BN) when $stripe = 2$. The resolution, denoted by the letter r in Figure 3, is just the characteristic matrix's height and width. The input and output, r , are unaltered when the step distance, s , equals 1; the output, r , is half of the input when $s = 2$. g denotes the group width of each group in the group convolution, b denotes the bottleneck ratio, which means that the channel of the output characteristic matrix is reduced to

$1/b$ of the input characteristic matrix channel, and W is the characteristic matrix's channel.

A straightforward formula that makes use of the parameters W_0, W_a and W_m can be used to calculate the width of the layers in RegNet. The following formula can be used to get the width at a specific stage, i is:

$$W_i = [W_0 + W_a \cdot \frac{i}{W_m}] \quad (9)$$

Where, W_i is the width of the i th stage, W_0 is the starting width, W_a is the width growth and W_m is the width multiplier the floor function is represented by $[\cdot]$, which rounds to the closet integer.

3.4

3.5 Segmentation

When an image is categorized as "Abnormal," a Dual Attention V-Network is used for additional processing. With this network, the tumor region may be precisely segmented, giving a thorough outline of the brain tumor. The network is made to focus on various areas of the image. The Dual Attention V-Network integrates the spatial attention and channel attention mechanisms—two essential mechanisms frequently employed in visual tasks—to capture intricate relationships and improve feature representation. By enabling the network to concentrate on the most informative portions of the input, these two attention processes enhance its performance in tasks like as object detection, segmentation, and image classification. Figure 4 displays the Dual Attention V-Network architecture,

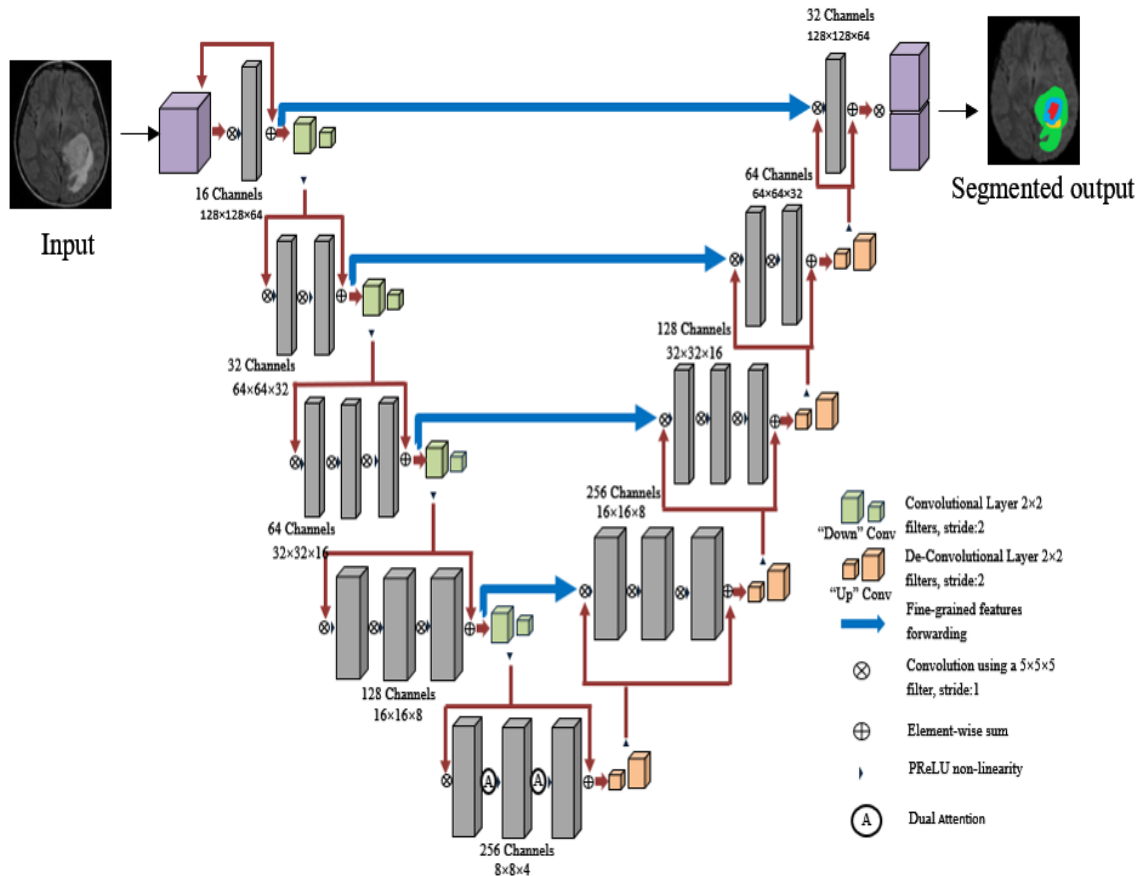


Figure 4: The architecture of Dual Attention V-Network

i) Spatial Attention Mechanism

The significance of various spatial locations is the focus of spatial attention. The spatial attention mechanism represented mathematically,

$$SA(F) = \sigma(Conv([AvgPool(F); MaxPool(F)])) \quad (10)$$

F is the input feature map in this case. In order to create spatial maps, AvgPool and MaxPool stand for global average pooling and global max pooling along the channel axis. A convolutional operation is called conv. The sigmoid activation function is denoted by σ . To recalibrate the spatial features, multiply the resulting spatial attention map by the input feature map.

ii) Channel Attention Mechanism

The significance of various feature maps is the focus of channel attention. The channel attention process expressed mathematically,

$$CA(F) = \sigma(MLP(AvgPool(F)) + MLP(MaxPool(F))) \quad (11)$$

F is the input feature map in this case. Global max pooling is represented by MaxPool, while global average pooling is represented by AvgPool. Multi-Layer Perceptrons, or MLPs for short, usually have two fully connected layers. The sigmoid activation function is denoted by σ . To recalibrate the channels, the input feature map is multiplied by the weighted vector that is the output.

iii) Dual Attention V-Network

These two attention methods are integrated in the Dual Attention V-Network to improve the feature maps:

$$F' = SA(F) \times (CA(F) \times F) \quad (12)$$

where the initial feature map is denoted by F. The channel attention recalibrated feature map is denoted as CA(F). The spatial attention recalibrated feature map is called SA(F). These attention-enhanced feature maps are multiplied element-wise to produce the final output F', which improves feature representation. The network can now choose highlight significant elements in both the spatial and channel dimensions as a result to this combination.

4. RESULTS AND DISCUSSION

This section presents the evaluation of the proposed BTS-VNET using four datasets, applying a number of measures consist of recall, precision, specificity, accuracy and f1 score. Benchmark includes the operation of the proposed result as well as the complete accuracy rate which has been carefully defined and evaluated.

4.1 Performance metrics

A proposed BTS-VNET can be assessed based on FScore, average sensitivity, time taken, segmentation accuracy (SA), average misclassification ratio (AMR), average F1 score, average time taken, average segmentation accuracy and eye perception-based quality index (EPQI).

$$F1\ score = 2 \left(\frac{Precision \times Recall}{Precision + Recall} \right) \quad (13)$$

$$Precision = \frac{T_{pos}}{T_{pos} + F_{pos}} \quad (13.1)$$

$$Recall = \frac{T_{pos}}{T_{pos} + F_{neg}} \quad (13.2)$$

$$Sensitivity = \frac{T_{pos}}{T_{pos} + F_{pos}} \quad (14)$$

$$SA = 2 \left(\frac{T_{pos} + T_{neg}}{T_{pos} + F_{pos} + T_{neg} + F_{neg}} \right) \times 100 \quad (15)$$

$$AMR = \frac{F_{pos} + F_{neg}}{T_{pos} + T_{neg} + F_{pos} + F_{neg}} \quad (16)$$

Where T_{neg} and T_{pos} specifies true negatives and true positives of the sample images, F_{neg} and F_{pos} specifies false negatives and false positives of the sample images.

4.1.1 Analysis on F1 Score

The FScore is a metric used to analyse the quality of binary segmentation or multi-class segmentation in brain MRI images. This metric is constructed by combining the precision and recall functions in image segmentation. The precision metric is calculated by the division of the true positive count by the sum of the true positive and false positive. The recall metric is calculated through dividing the true positive count by the sum of true positive and false negative.

Table 1: FScore analysis for brain tumor segmentation

| Database | FScore | | | |
|----------|---------|---------|-----------|-------------------|
| | Method | | | |
| | BCS-SRN | BCS-GED | BCS-HSCRD | Proposed BTS-VNET |
| MMHRC-DB | 0.8900 | 0.8938 | 0.8962 | 0.9260 |
| PRNV-DB | 0.8949 | 0.9088 | 0.9072 | 0.9458 |
| NSC-DB | 0.8909 | 0.8938 | 0.9026 | 0.9219 |
| SSL-DB | 0.8906 | 0.8927 | 0.9080 | 0.9449 |

Table 1 portray the detailed FScore analysis for brain tumor segmentation. The analysis is based upon four methods such as BCS-SRN, BCS-GED, BCS-HSCRD, and the proposed BTS-VNET method. For this analysis, the databases MMHRC-DB, PRNV-DB, NSC-DB, and SSL-DB are used. From this table, the proposed BTS-VNET method holds a higher FScore value than the existing methods, viz. BCS-SRN, BCS-GED, and BCS-HSCRD. Also, the PRNV-DB database provides a better FScore value than the other three databases.

4.1.2 Analysis on Average Sensitivity

The sensitivity metric measures the rate of actual positive values, which are correctly identified as brain tumor pixels. The range of sensitivity lies between 0 and 1. The high-scored sensitivity denotes the best cancer segmentation method, and vice-versa.

Table 2: Avg. sensitivity analysis on brain tumor segmentation

| Database | Avg. Sensitivity | | | |
|----------|------------------|---------|-----------|-------------------|
| | Method | | | |
| | BCS-SRN | BCS-GED | BCS-HSCRD | Proposed BTS-VNET |
| MMHRC-DB | 0.8939 | 0.8922 | 0.9007 | 0.9110 |
| PRNV-DB | 0.8963 | 0.8991 | 0.9052 | 0.9112 |
| NSC-DB | 0.8892 | 0.8962 | 0.8992 | 0.9203 |
| SSL-DB | 0.8922 | 0.8928 | 0.9046 | 0.9270 |

Table 2 focus on the average sensitivity analysis of brain tumor segmentation. Herein, the considered methods are BCS-SRN, BCS-GED, BCS-HSCRD, and the proposed BTS-VNET. From the table, the proposed BTS-VNET method holds a higher sensitivity value than the existing methods, namely BCS-SRN, BCS-GED, and BCS-HSCRD.

4.1.3 Analysis on Time Taken

The time taken analysis incorporates the methods BCS-SRN, BCS-GED, BCS-HSCRD, and the proposed BCS-XYZ. While taking segmentation into account, the time taken for segmentation is inversely proportional to the computational speed. Hence, reducing the time taken gives faster computation. The unit of time is measured in terms of *Seconds*.

Table 3: Time Taken analysis for brain tumor segmentation

| Database | Time taken (in Sec) | | | |
|----------|---------------------|---------|-----------|-------------------|
| | Method | | | |
| | BCS-SRN | BCS-GED | BCS-HSCRD | Proposed BTS-VNET |
| MMHRC-DB | 23.73 | 20.57 | 20.03 | 17.28 |
| PRNV-DB | 20.67 | 20.44 | 19.82 | 17.46 |
| NSC-DB | 23.32 | 20.83 | 20.24 | 17.14 |
| SSL-DB | 22.80 | 20.69 | 19.85 | 17.33 |

Table 3 express the time-taken analysis of brain tumor segmentation methods. From the table PRNV-DB is considered as the best supportive database regarding the run time. The highest time consumption (i.e., 23.73 sec) is absorbed by the BCS-SRN method which declares the BCS-SRN method is the least efficient one for execution time cost.

4.1.4 Analysis on Segmentation Accuracy

Segmentation accuracy (SA) is the quality measure of cancer object segmentation algorithm using the four parameters TP, FP, FN, and True Negative (TN), which is measured in the unit of percentage (%). Segmentation accuracy computes the segmentation quality by considering the correctness of both the cancer object region and the background region. The high-scored SA points out the better segmentation algorithm and vice-versa.

Table 4: Segmentation accuracy analysis for brain tumor segmentation

| Database | Segmentation Accuracy (%) | | | |
|----------|---------------------------|---------|-----------|-------------------|
| | Method | | | |
| | BCS-SRN | BCS-GED | BCS-HSCRD | Proposed BTS-VNET |
| MMHRC-DB | 91.20 | 91.28 | 92.47 | 95.22 |
| PRNV-DB | 91.35 | 91.76 | 92.88 | 95.65 |
| NSC-DB | 90.60 | 90.95 | 91.60 | 93.31 |
| SSL-DB | 91.02 | 91.32 | 92.13 | 94.70 |

Table 4 focus on the segmentation accuracy analysis for brain tumor segmentation. From the table the proposed method has the highest percentage of segmentation accuracy than the existing BCS-SRN, BCS-GED, and BCS-HSCRD methods. The BCS-XYZ method achieves a segmentation accuracy of 95.65% on the PRNV-img image from the PRNV-DB database. This high accuracy rate confirms the effectiveness of the proposed method.

4.1.5 Analysis on Average Misclassification Ratio

The Average Misclassification Ratio (AMR) measures the ratio of pixels that are wrongly predicted as either cancer objects or background.

Table 5: AMR analysis for brain tumor segmentation

| Method | Avg. Misclassification Ratio | | | |
|-------------------|------------------------------|---------|--------|--------|
| | Database | | | |
| | MMHRC-DB | PRNV-DB | NSC-DB | SSL-DB |
| BCS-SRN | 0.09 | 0.08 | 0.09 | 0.09 |
| BCS-GED | 0.08 | 0.08 | 0.08 | 0.09 |
| BCS-HSCRD | 0.07 | 0.07 | 0.07 | 0.08 |
| Proposed BTS-VNET | 0.05 | 0.04 | 0.05 | 0.06 |

Table 5 deliver the analysis report on the average misclassification ratio for the four methods, namely BCS-SRN, BCS-GED, BCS-HSCRD, and the proposed BTS-VNET. The proposed BTS-VNET method, which has the lowest misclassification ratio of 0.04 on the PRNV-DB database, is considered the best segmentation method. On the other hand, the existing BCS-SRN method has the highest misclassification ratio of 0.09 on the NSC-DB database. Consequently, the BTS-VNET method demonstrates superior classification accuracy compared to the BCS-SRN method.

4.4.9 Analysis on Eye Perception based Quality Index

Eye Perception based Quality Index (EPQI) analysis is drawn based on the human perception. Herein, the quality of each brain tumor segmentation method is inspected by 10 human observers. Based on their human eye perception, each segmentation methodology is allocated by index values.

Table 9: EPQI analysis for brain tumor segmentation

| Database | EPQI | | | |
|----------|---------|---------|-----------|-------------------|
| | Method | | | |
| | BCS-SRN | BCS-GED | BCS-HSCRD | Proposed BTS-VNET |
| MMHRC-DB | 1 | 2 | 3 | 4 |
| PRNV-DB | 1 | 2 | 3 | 4 |
| NSL-DB | 1 | 2 | 3 | 4 |
| SSL-DB | 1 | 2 | 3 | 4 |

Table 9 focus on the Eye Perception based Quality Index (EPQI) analysis using the methods BCS-SRN, BCS-GED, BCS-HSCRD, and the proposed BCS-XYZ. Generally, in EPQI analysis which is constituted by four research methods, the best quality segmentation method is allocated with the index value 4. The second-quality segmentation is allocated with the index value 3. The third-quality segmentation is allocated with the index value 2. The least-quality segmentation method is allocated by the index value 1. The EPQI analysis proves the efficiency of the proposed BTS-VNET method than the existing methods for brain tumor segmentation.

5. CONCLUSION

In this research, BTS-VNET model has been proposed for brain tumor segmentation. The input images are gathered from the image datasets. The process begins with input MRI scans that undergo pre-processing steps, including skull stripping and scalable range based adaptive bilateral filter (SCRAB) for removing the noisy artifacts. The pre-processed images are then passed through a Dilated Regularized Network for initial tumor detection for classifying the MRI images as either normal or abnormal. Afterwards, the abnormal images are fed into the tumor detection segmentation phase using a Dual Attention V-Net for resulting in segmented output that segments different tumor regions. Different sub-compartments of the tumor such as enhanced tumor, edema, non-enhanced tumor and necrosis are segmented. The proposed method is evaluated in terms of FScore, sensitivity, time taken, segmentation accuracy, average misclassification ratio, and eye perception-based quality index (EPQI). According to the experiment, the proposed method has 95.65% accuracy in brain tumor segmentation.

References

1. Sai Meghana, S., Amulya, P., Manisha, A. and Rajarajeswari, P., 2019. A deep learning approach for brain tumor segmentation using convolution neural network. *International Journal of Scientific and Technology Research*, 8(12), pp.1697-1702.
2. Khan, M.F., Iftikhar, A., Anwar, H. and Ramay, S.A., 2024. Brain Tumor Segmentation and Classification using Optimized Deep Learning. *Journal of Computing & Biomedical Informatics*, 7(01), pp.632-640.
3. Amin, J., Sharif, M., Raza, M. and Yasmin, M., 2024. Detection of brain tumor based on features fusion and machine learning. *Journal of Ambient Intelligence and Humanized Computing*, pp.1-17.

4. Liu, Z., Tong, L., Chen, L., Jiang, Z., Zhou, F., Zhang, Q., Zhang, X., Jin, Y. and Zhou, H., 2023. Deep learning-based brain tumor segmentation: a survey. *Complex & intelligent systems*, 9(1), pp.1001-1026.
5. Balamurugan, T. and Gnanamanoharan, E., 2023. Brain tumor segmentation and classification using hybrid deep CNN with LuNetClassifier. *Neural Computing and Applications*, 35(6), pp.4739-4753.
6. Lamrani, D., Cherradi, B., El Gannour, O., Bouqentar, M.A. and Bahatti, L., 2022. Brain tumor detection using mri images and convolutional neural network. *International Journal of Advanced Computer Science and Applications*, 13(7).
7. Almadhoun, H.R. and Abu-Naser, S.S., 2022. Detection of brain tumor using deep learning.
8. Mushtaq, S., Roy, A. and Teli, T.A., 2021. A comparative study on various machine learning techniques for brain tumor detection using MRI. *Proc. of the Global Emerging Innovation Summit (GEIS-2021)*, pp.125-137.
9. Ding Y., Chen F., Zhao Y., Wu Z., Zhang C. and Wu D., 2019, 'A Stacked Multi-Connection Simple Reducing Net for Brain Tumor Segmentation' *IEEE Access*, vol. 07, pp. 104011-104024.
10. Gawad A.H.A., Said A.L. and Radwan A.G., 2020, 'Optimized Edge Detection Technique for Brain Tumor Detection in MR Images', *IEEE Access*, vol. 08, pp. 136243-136259.
11. Gunasekara, S.R., Kaldera, H.N.T.K. and Dissanayake, M.B., 2021. A systematic approach for MRI brain tumor localization and segmentation using deep learning and active contouring. *Journal of Healthcare Engineering*, 2021(1), p.6695108.
12. Jia, Z. and Chen, D., 2020. Brain tumor identification and classification of MRI images using deep learning techniques. *IEEE Access*.
13. Khan, A.H., Abbas, S., Khan, M.A., Farooq, U., Khan, W.A., Siddiqui, S.Y. and Ahmad, A., 2022. Intelligent model for brain tumor identification using deep learning. *Applied Computational Intelligence and Soft Computing*, 2022(1), p.8104054.
14. Ejaz K., Rahim M.S.M., Bajwa U.I., Chaudhry H., Rehman A. and Ejaz F., 2021, 'Hybrid Segmentation Method With Confidence Region Detection for Tumor Identification', *IEEE Access*, vol. 09, pp. 35256-35278..
15. Yaqub, M., Feng, J., Zia, M.S., Arshid, K., Jia, K., Rehman, Z.U. and Mehmood, A., 2020. State-of-the-art CNN optimizer for brain tumor segmentation in magnetic resonance images. *Brain Sciences*, 10(7), p.427.
16. ZainEldin, H., Gamel, S.A., El-Kenawy, E.S.M., Alharbi, A.H., Khafaga, D.S., Ibrahim, A. and Talaat, F.M., 2022. Brain tumor detection and classification using deep learning and sine-cosine fitness grey wolf optimization. *Bioengineering*, 10(1), p.18.
17. Vankdothu, R. and Hameed, M.A., 2022. Brain tumor MRI images identification and classification based on the recurrent convolutional neural network. *Measurement: Sensors*, 24, p.100412.
18. Guan, Y., Aamir, M., Rahman, Z., Ali, A., Abro, W.A., Dayo, Z.A., Bhutta, M.S. and Hu, Z., 2021. A framework for efficient brain tumor classification using MRI images.
19. Nassar, S.E., Yasser, I., Amer, H.M. and Mohamed, M.A., 2024. A robust MRI-based brain tumor classification via a hybrid deep learning technique. *The Journal of Supercomputing*, 80(2), pp.2403-2427.
20. Kumaar, M.A., Samiayya, D., Rajinikanth, V., Raj Vincent PM, D. and Kadry, S., 2024. Brain tumor classification using a pre-trained auxiliary classifying style-based generative adversarial network.
21. Chauhan, A.S., Singh, J., Kumar, S., Saxena, N., Gupta, M. and Verma, P., 2024. Design and assessment of improved Convolutional Neural Network based brain tumor segmentation and classification system. *Journal of Integrated Science and Technology*, 12(4), pp.793-793.
22. MMHRC Database, 2021, Accessed from <<https://www.mmhrc.in/>>, Accessed on [5 Aug 2022].
23. PRNV Database, 2021, Accessed from <<https://www.teleradiologyhub.com/diagnostics/details/36/927-prnav-diagnostics-centre>>, Accessed on [5 Aug 2022].
24. NSC Database, 2021, Accessed from <<https://nagercoilscancentre.business.site/>>, Accessed on [5 Aug 2022].
25. SSL Database, 2021, Accessed from <<https://www.saravanascons.com/>>, Accessed on [5 Aug 2022].